N92-14080

COBE GROUND SEGMENT GYRO CALIBRATION

I. Freedman, V.K. Kumar, A. Rae, R. Venkataraman (ST Systems Corporation [STX], Lanham, MD 20706),
F.S. Patt (General Sciences Corporation [GSC], Laurel, MD 20707),
E.L. Wright (UCLA, Los Angeles, CA 90024-1562)

ABSTRACT

This paper discusses calibration of the scale factors and rate biases for the Cosmic Background Explorer (COBE) spacecraft gyroscopes, with emphasis on the adaptation for COBE of an algorithm previously developed for the Solar Maximum Mission (SMM). Detailed choice of parameters, convergence, verification, and use of the algorithm in an environment where the reference attitudes are determined from the Sun, Earth, and star observations (via the Diffuse Infrared Background Experiment [DIRBE]) are considered. Results of some recent experiments will be shown. These include tests where the gyro rate data are corrected for the effect of the gyro baseplate temperature on the spacecraft electronics.

1. INTRODUCTION

This paper presents the results of a successful implementation of a gyro calibration system for support of the ongoing Cosmic Background Explorer (COBE) mission. The algorithm has been previously implemented successfully in the High-Energy Astrophysical Observatory (HEAO), SMM, and (most recently) Hubble Space Telescope (HST) projects. The application for COBE is in support of final aspect determination for the production of the Project Data Sets in the Cosmology Data Analysis Center (CDAC). The COBE attitude profile is unique and thus imposes constraints and demands on the calibration algorithm that have not been encountered in prior applications.

The scope of this paper is somewhat unusual in that it combines the implementation and theoretical verification of the calibration system with the analysis of results and practical limitations based on the flight data. A coauthor (Freedman) performed substantial verification of the algorithm based purely on mathematical analysis and verified these conclusions using simulated data following implementation. Another (Patt) relied upon hands-on experience with past calibration applications to explore the practical limitations of the algorithm using the flight data and to thoroughly exercise the system in a variety of on-orbit situations. In doing so, we discovered the surprisingly dynamic behavior of the gyro temperature and the substantial impact that it has on the calibration stability.

The paper has been organized as follows: Section 1 summarizes the need for gyro calibration in the aspect determination and the choice of the algorithm. Section 2 presents the implementation details and the preflight verification. Section 3 discusses the results of the actual calibration using the flight data. Section 4 summarizes the results and discusses the human interface.

1.1 THE NEED FOR GYRO CALIBRATION IN THE COBE GROUND SEGMENT

The final aspect determination for the COBE mission depends critically on the accuracy of the gyro-propagated attitude. This is especially true for the DIRBE Fine Aspect determination; because the DIRBE star sightings occur on the average once per minute, the gyro propagation is the critical link that spans the time between observations and allows a number of observations to be incorporated into a single solution. Even for the Coarse Attitude determination, which has much less stringent requirements, the gyro propagation provides substantial smoothing of the solutions and minimizes the effects of sensor quantization errors, misalignments, and unmodeled systematic errors. Although at some point the gyro attitude propagation will inevitably degrade because of gyro noise and digitization errors, the accuracy of propagation depends to a large degree on the quality of the gyro calibration.

1.2 THE CHOICE OF THE CALIBRATION ALGORITHM

The SMM gyro calibration algorithm (Ref. 1) was chosen over in-line (i.e., integral to the attitude determination process) algorithms based on the following factors:

- This algorithm, which was originally developed at Goddard Space Flight Center (GSFC) by Mr. P. Davenport, has been thoroughly flight-tested on previous Center projects. It is well known to one coauthor (Patt), who has used it successfully on the SMM and previous missions.
- Input to the algorithm consists of attitude quaternions and angular velocities so it is independent of sensor data type and may be used with Fine Aspect solutions.
- It is compatible with the use of the Quest algorithm and with batch-least-squares attitude algorithms, which had already been designed into the COBE ground segment.
- The algorithm is linear in the complete set of gyro calibration parameters: scale factor corrections, misalignments, and biases. It readily supports user selection of the solve-for parameter subset, and it allows for analytical determination of parameter visibility.
- It has no inherent limitations on the number of attitude solutions that can be incorporated into the calibration and therefore can use an arbitrary time span of data.
- It can be fully automated using the existing file structure in the COBE Attitude software system. Its design as an adjunct to the software rather than an integral part is consistent with the philosophy of automated pipeline processing and supports its use as a quality assurance tool.

2.1 ALGORITHM DESCRIPTION

Following the presentation in Ref. 1 (which contains more detail), we note that any rate gyro assembly (RGA) must be composed of at least three gyroscopes whose axis directions taken together completely span the space of possible rotations.

An RGA consisting of three gyros will produce as a response a "vector" $\bar{R}$ of responses of individual gyros whose sensitive axes are $\hat{u}_i$ (i=1,2,3) in the spacecraft body frame. This response vector is translated into a measured angular velocity $\bar{W}_M$ in the body frame via the relation

$$\bar{W}_M = \tilde{G}_0\bar{R} - \bar{D}_0 \qquad [1]$$

where $\tilde{G}_0$ is the RGA 3 x 3 scale-factor/alignment matrix and $\bar{D}_0$ is the drift rate bias.

$\tilde{G}_0$ is related to the scale factors k_i and gyro alignments $\hat{u}_i$ by the equation

$$\tilde{G}_0 = (1 + k_i)\hat{u}_i, \ (i=1,2,3). \qquad [2]$$

If $\tilde{G}_0$ and $\bar{D}_0$ deviate from their true values, either because of poor initial calibration or because of temporal changes in the RGA, $\bar{W}_M$ will differ from the true angular rate $\bar{W}$. The goal of the algorithm is to determine correction matrices $\tilde{M}$ and $\bar{d}$ that may be applied to $\tilde{G}_0$ and $\bar{D}_0$ so that a modified equation [1] will yield the true angular rate:

$$\tilde{G} = \tilde{M}\,\tilde{G}_0;\ \bar{D} = \tilde{M}\,\bar{D}_0 + \bar{d};\ \bar{W} = \tilde{G}\bar{R} - \bar{D} = \tilde{M}\bar{W}_M - \bar{d} \qquad [3]$$

The angular rate deviation $\bar{w}$ between the measured and true rates is given by

$$\bar{w} = \bar{W}_M - \bar{W} = -\tilde{m}\bar{W}_M + \bar{d} \qquad [4]$$

where $\tilde{m} = \tilde{M} - \tilde{I}$ and $\tilde{I}$ is the identity matrix. The algorithm will solve for $\tilde{m}$ and $\bar{d}$, separately or together. Because the RGA we are considering contains exactly three gyros, $\tilde{m}$ and $\bar{d}$ contain sufficient information to allow separate calibration updates of scale factor alignment and drift for the individual gyros.

The rotation from the RGA-determined end-of-interval attitude to the true end-of-interval attitude transformed to the start-of-interval reference frame may be determined. The vector part of this rotation quaternion, $\bar{Z}_n$ for the nth calibration interval is given by equation [13] of Ref. 1 under the approximations that the rotation determined from the RGA is in agreement with the true rotation to the first order in the error and that the error rotation angle is sufficiently small that the cosine may be approximated by 1 (i.e., the fourth component of error quaternion is 1).

$$\bar{Z}_n = -1/2\int[\tilde{T}_n(\tilde{m}\bar{W}_M - \bar{d})], \; n = 1,2...N. \qquad [5]$$

Here $\tilde{T}_n$ is the matrix for transforming vectors to start-of-interval spacecraft body coordinates.

Equation [2.1-5] is linear in the unknowns $\tilde{m}$ and $\bar{d}$ and lends itself naturally to standard least-squares techniques.

Following equation (4-182) of Ref. 2, this rotation may also be written as

$$\bar{Z}_n = \textit{vector portion of } \{q_0\, q_{I0}^*\, q_{IK}\, q_K^* - I\}_n \qquad [6]$$

where q_0 and q_K are the propagated attitudes at the start and end of the calibration interval, and q_{0K} and q_{IK} are the reference attitudes, respectively. The $*$ denotes a quaternion conjugate.

The matrix equation that represents this equation applied to N calibration intervals is written as

$$\tilde{Z} = \tilde{H}\,\bar{x} \qquad [7]$$

where $\tilde{Z}$ and the state vector $\bar{x}$ are defined as

$$\tilde{Z} = \{Z_1^T,\, Z_2^T, \ldots, Z_N^T\}^T,$$
$$\bar{x} = 1/2\,(m_{11},\, m_{12},\, m_{13},\, m_{21},\, m_{22},\, m_{23},\, m_{31},\, m_{32},\, m_{33},\, d_1,\, d_2,\, d_3)$$

and H is a 3N x 12 matrix determined by equation [5] above.

The linear "Bayesian" weighted least-squares loss function J may be used to place appropriate relative emphasis on a priori known calibration values and the updated values as

$$J = 1/2\,[E^T\,\tilde{W}\,E + (\bar{x}-\bar{x})_a^T\,\tilde{S}_a\,(\bar{x}-\bar{x})_a] \qquad [8]$$

$$\textit{where } E = \tilde{Z} - \tilde{H}\,\bar{x}_a$$

$\tilde{W}$ and $\tilde{S}_a$ are symmetric nonnegative definite weighting matrices and $\bar{x}_a$ is an a priori estimate of $\bar{x}$.

The gradient minimization approach applied to equation [7] yields the following equations for the state-vector x of corrections to the drift rates and biases:

$$[A]_{12 \times 12} \quad x_{12 \times 1} = y \qquad [9]$$

$$A = \tilde{S}_a + \tilde{H}\,\tilde{W}\,\tilde{H}^T;\ \bar{y} = \tilde{H}\,\tilde{W}\,\bar{Z}^T + \tilde{S}_a\,x_a$$

The A matrix above may be partitioned into submatrices as below:

$$A = \begin{bmatrix} A_{11} & A_{12} \\ A_{21} & A_{22} \end{bmatrix}$$ where A is a 9 x 9 matrix, and A_{12}, A_{21}, and A_{22} are 3 x 3.

For scale-factor calculation alone, A_{12} and A_{21} are zero. Thus, scale-factor and bias may be separately computed.

The solved-for scale-factors are related to the solved-for $\tilde{G}$ matrix by

$$(1+k)_i\ \hat{u}_i = |G_i| \text{ where } G_i \text{ is the } i^{th} \text{ row-vector of } \tilde{G}. \qquad [10]$$

Application of this algorithm to COBE demands consideration of the following:

COBE has three 2-axis gyro packages, each of which contains one gyro closely aligned to the A, B, or C control axes 120° apart in a plane, and one loosely aligned to the (orthogonal) spacecraft X axis. At any one time, data from one X-axis gyro only are included in the processing. The B control-axis gyro failed early in the mission, leaving the A and C control-axis gyros to support the mission. Because we do not have observability on all the gyro misalignments, the sensitive axis unit vectors were fixed at the prelaunch values throughout the mission.

The input to this algorithm consists of the gyro sample rate T = 1 second, the reference attitude quaternions q_{R0} and q_{RK} at the beginning and end of a calibration interval respectively, the measured angular velocities, and the duration of a calibration interval, which consists of n equally spaced samples. The entire data set consists of N calibration intervals. At least four calibration intervals are required to compute a scale-factor. One interval is sufficient to compute a bias. Our implementation accepts only calibration intervals for which all gyro samples are present. A robust matrix inversion technique (Singular Value Decomposition) was used to solve the calibration equations.

Requirements of better than 3 arcminutes RMS residuals with up to 45-min smoothing intervals demanded the use of 1-sec gyro samples to compute the propagated attitudes multiplicatively in double precision arithmetic. COBE rotates through approximately 4.8° per second about the X axis, and it proved to be insufficiently accurate to interpolate the 4-sec sampling rate attitude solutions to obtain adequate angular velocities. Gyro noise effects were not significant in batches as long as 45 minutes.

Previous missions to which this algorithm has been applied carry an independent attitude sensor that yields reference attitudes at commanded times considerably more accurate than is required of the overall solution, often as commanded maneuvers.

The only formal attitude maneuvers in the early mission useful for calibration were the spin-up/roll-slew data, which are discussed in Section 3.

COBE has no star-tracker, but data from the ongoing DIRBE star observations may be used to differentially correct QUEST solutions obtained from batch estimates of the attitude from Earth and Sun sensors (see Ref. 3).

Comparison of the single-frame with gyro-smoothed attitude solutions demonstrated the attitude propagation discontinuites at the smoothing interval boundaries. Numerical experiments showed that the QUEST solutions were appropriate for reference attitudes and should be determined without interpolation. The QUEST solutions themselves

depend on the accuracy of sensor observation propagation for synchronization (Ref. 3), so an iterative approach, "calibrate—determine QUEST solutions—recalibrate," was applied.

A null initial parameter set led to very slow or nonconvergence with oscillation over many iterations. Convergence required a starting approximation so that the correction was small. An initial parameter set was therefore obtained from the manual adjustment of the X-axis gyro scale factors and rate biases as described in Section 3.

The integrated difference rotation between reference and propagated attitudes was << 180° over the calibration interval; thus, ambiguities and aliasing problems were avoided.

The attitude accuracy is isotropic (given several star-sightings), so the observation weights ($\bar{W}$) were chosen to be identity matrices.

An "optimal" choice for the state vector weight matrix ($\bar{S}_o$) is the inverse of the normalized solution covariance matrix. These weights are updated at each iteration.

This weighting scheme—in terms of the inverse of covariance matrices—is proportional to the inverse of the A matrix described above; an order of magnitude estimate of A_{11}^{-1} will be made in Section 2.3.

2.2 SIMULATED DATA TESTS

Simulated sinusoidal 3-axis attitudes with constant scale factor and alignment matrices and rate biases at constant vector angular velocity were used to verify the implementation.

Table 1 shows that the input and recovered scale-factors and biases agree to several significant figures.

A sensitivity study performed with kinematically simulated data showed the expected proportional sensitivity to scale-factor errors.

2.3 IMPLEMENTATION CHECK

Analytic expressions for every quantity of the algorithm were derived for detailed checks in the special case where the reference attitudes are the transformation at the interval endpoints, combined with constant uniaxial angular velocity and scale-factor-and-alignment matrix. The observation weights were chosen to be identity matrices, and no a priori knowledge of the parameters was assumed.

This study led to order of magnitude estimates for the calibration equations in the notation of Ref. 1.

$$A_{11}(1,1)=1+N(Wn)^2$$

$$A_{11}(2,2)=1$$

$$A_{11}(3,3)=1$$

$$A_{12}(1,1)=-(Wn^2) \qquad [11]$$

$$A_{22}(2,2)=n^2$$

$$y_1(1)=(NWn)\ \sin\ (WnT/2)$$

$$Y_2(1)=(NWn)\ \sin\ (WnT/2)$$

Table 1. Tests of Gyro Calibration Algorithm Using Simulated Data

Test #	Description	Result
Tests using simulator		
In each case - 800 second smoothing interval, 4 smoothing intervals of data sampled at 4 second intervals		
NULL TEST		
1.	No gyro calibration errors in input attitudes	Successful - the scale factor and biases were computed as zeroes
SCALE-FACTOR DETERMINATION		
- X-AXIS SPIN ONLY		
2.	-4.8 deg/sec spin about X axis; X scale-factor error=1.2e-3; state vector was weighted to determine X scale-factor only	Successful - the computed X scale-factor = 1.2e-3
3.	Similar to case-2; X scale-factor error was set to 1.6e-3	Successful - the computed X scale-factor = 1.6e-3
4.	Similar to case-2; X scale-factor error was set to 0.2 (a large value)	Successful - the computed X scale-factor = -1.6e-2 (aliased as more than 360 deg rotation between reference attitudes)
- SWITCH X-AXIS GYRO IN SOFTWARE		
5.	As case-3, but using BX or CX gyros	Successful - we were able to switch X axis gyros in software.
- TRANSVERSE AXIS SPIN PROJECTION		
6.	-4.8 deg/sec spin about Z-axis; scale-factor error was set to 1.2e-3 on Z-axis; A, C, AX gyros.	Successful - the computed A-axis scale-factor = 1.2e-3; - the computed C-axis scale-factor = 3.0e-4; (correct projection on C-axis)
7.	-4.8 deg/sec spin about C-axis; scale factor error set to 1.6e-3 on C-axis; A, C, AX gyros.	Successful - the computed C-axis scale-factor = 1.6e-3; - the computed A-axis scale-factor = 4.0e-4 (correct projection on A-axis)
BIAS DETERMINATION		
8.	-4.8 deg/sec spin about X-axis; bias set to 5.6e-4 deg/sec on X-axis; state-vector weighting permitted only bias determination; A,C, AX gyros.	Successful - the computed X-axis bias = 5.6e-4
- PROJECTION ON TRANSVERSE AXES		
9.	No spin; bias set to 8.0e-4 deg/sec about Y-axis; AX gyro only.	Successful - null result
10.	As case-9 but bias set to 8.0e-4 deg/sec about Z-axis; AX gyro only.	Successful - null result
11.	As case-9 but bias set to 8.0e-4 deg/sec about Z-axis; A, C, AX gyros.	Successful - computed A-axis bias = 5.0e-4 - computed C-axis bias = -3.0e-4 (correct projection on C-axis)

all other terms being zero, where N is the number of calibration intervals and n is the number of attitude samples per interval. W represents the observed angular velocity. T represents the duration of a calibration interval.

If we start with zero initial corrections, the calibration equations become:

$$A_m = A_{11} - A_{12} A_{22}^{-1} A_{12}^T = [1 + N(Wn)^2] + Wn^2 (1+n^2)^{-1} (-Wn^2), \qquad [12]$$

$$y_m = y_1 - A_{12} A_{22}^{-1} y_2 \text{ as above } (m=1,2,..,n),$$

where A_{22}^{-1} denotes the pseudo-inverse of the A_{22} submatrix.

These results were checked against the simulated values.

Note that the relative accuracy of propagation must be better than n^{-2} for adequate estimate of the calibration equations, and an "optimal" relative weighting of n^{-2} on the sensitive axis is indicated.

3.1 CHOICE OF PARAMETERS AND STATE VECTOR CONVERGENCE (FLIGHT DATA)

The choice of the state vector elements to be included in the solve-for parameter set was based on a combination of prelaunch analysis, simulation, and on-orbit verification of the calibration algorithm. The on-orbit results were obtained for two cases: the initial spin-up of the spacecraft, and the constant-spin, standard operational mode. The following subsections discuss the factors that limit state vector observability, followed by the methods and results for the two cases.

Limitations on State Vector Observability

The COBE attitude control configuration (spin about one axis at 0.8 RPM combined with precession about the Sun vector once per orbit) severely limits the observability of some gyro parameters and results in significant correlations among others. The details of these limitations are best explored via the detailed methods of analysis, simulation, and algorithm verification mentioned above; however, in a qualitative sense these results can be inferred intuitively, which provides a convenient means for summarizing the observability problem.

The COBE gyro configuration has one gyro aligned with the spin axis (there is onboard redundancy in this area, but only one spin axis gyro output can be telemetered) and two working gyros in the spin-normal plane, the redundant gyro in this plane having failed soon after launch. (The spacecraft axes in this plane are referred to as the control axes because they are used to control the spacecraft precession, or pitch, rate.) The control axis gyros are not orthogonal but are 120° apart. In the standard gyro calibration parameter set, each gyro is subject to a scale factor error, misalignments (measured as azimuth, or rotation about the spin axis, and elevation, or angle relative to the spin axis), and a constant rate error, or bias.

For the spin axis gyro, if the spin rate variations are small, the scale factor and bias are almost completely correlated; thus, one of these can be held constant. The effect of misalignments of this gyro is small, for two reasons: the effect of any misalignment is a small fraction of the orbit precession rate, which is itself smaller than the spin rate by a factor of 80, and the effect is cyclic and tends to integrate to zero each spin. Thus, for most of the mission only one term need be considered for this gyro. The exception, of course, was during the spin-up, when both the bias and scale factor could be evaluated.

The control axis gyro biases have an effect that is similar to the spin axis gyro misalignments: at the mission spin rate they contribute a small cyclic error that integrates to effectively zero over one spin. The elevation components of the misalignments result in an error that is a small fraction of the spin rate; in the mission mode this also amounts to a constant rate error, which, like the biases, is essentially unobservable. The biases and the elevation errors are thus highly correlated. (These parameters may be more visible at the lower spin rates from the early mission, and

this possibility had not been explored as of this writing.) The scale factors have reasonable observability because the control axis gyro output is essentially a sinusoidal modulation of the spacecraft pitch rate; in other words, errors in these scale factors would result in a pitch error that accumulates linearly. On the other hand, for an ideal (wobble-free) control system, the control axis scale factors are completely correlated; the extent to which these are individually observable depends on the nonuniformity of the pitch rate, the spin axis wobble, and the spin rate. The azimuth alignment errors in these gyros have observability and correlation characteristics that are essentially identical to those of the scale factors because they contribute to an accumulation of error about an axis perpendicular to the pitch axis.

Weighting Scheme and Convergence Criteria

The algorithm allows for the observation and state vectors each to be independently weighted. For the COBE calibrations we chose to use observation weights of unity and to use relative values for the state weights; in fact, based on the estimated solution accuracy, the true observation weights would have been approximately 1.E+6 for the Coarse attitudes and 4.E+6 for the Fine Aspect. Therefore, the state weights were reduced by about 1.E+6 from values based on the estimated uncertainties, and evaluations of the state vector observability using the calibration algorithm were performed by reducing the variances by the same factor. Thus, for example, a bias correction of 1.E-6 was considered significant only if the square root of the variance was 1.E-3 or less.

The state weights for the solve-for parameters were typically set at unity in the first iteration, equivalent to uncertainties of about 1.E-3. The weight for the spin-axis gyro bias was generally left at this value, although the uncertainty was usually much smaller because the observability of this parameter was very good. The weights for the other parameters would typically be increased after each iteration, depending on the magnitude of the correction and its estimated effect on the attitude propagation errors. The best example of this is given in the following section.

As stated previously, the calibration algorithm is very linear, but only to the extent that the calibration errors in the current iteration did not affect the accuracy of the attitude solutions used for the next iteration. For the COBE attitude profile the propagation errors do not accumulate linearly with time; thus, even the attitudes at the midpoints of the gyro propagation intervals were affected by the calibration errors. Therefore, it was necessary to iterate on the calibration if the errors in the a priori state vector were not small. The convergence criteria were selected for each parameter based on its effect on the overall propagation accuracy relative to the Fine Aspect specification; the criteria were 1.E-6 for the spin axis scale factor, 1.E-5 for the spin axis bias, and 1.E-4 for the control axis scale factors.

Gyro Calibration During the Spacecraft Spin-Up

The COBE spin rate was increased from its initial value of 0.23 RPM to the mission mode rate of 0.82 RPM in three roughly equal steps, at 1-day intervals (November 25, 26, and 27, 1989). This activity provided the only opportunity to separately calibrate the spin axis gyro scale factor and bias; it also provided excellent visibility on the individual control axis scale factors.

The following table illustrates the convergence of the state vector. The a priori values were chosen to be 1.E-3 for the spin axis scale factor correction (based on the experience with manual adjustments to the scale factor) and zero for all other parameters.

Iteration	X Scale Factor	X Bias (deg/sec)	A Scale Factor	C Scale Factor
A Priori	1.0E-3	0.0	0.0	0.0
1	1.060E-3	4.7E-4	1.96E-3	0.0
2	1.066E-3	5.2E-4	1.96E-3	-0.34E-3
3	1.066E-3	5.2E-4	1.96E-3	-0.46E-3

The initial weights were chosen to be unity for the solve-for parameters (for the control axis gyros this included the scale factors and azimuth misalignments; because of the nonorthogonal transformation between the control gyro and

the spacecraft axes, the scale factor and azimuth corrections are coupled in the calibration; the misalignments corrections were insignificant) and 1.E+4 for all other parameters. At each iteration, the weights for the updated parameters were increased by a factor of 100, except for the spin (X) axis bias, which was allowed to "float." The convergence was very rapid for the spin (X) axis parameters, with about 90% of the residual error being removed at each step. The A gyro scale factor also converged rapidly. The correction to the C gyro was small in the first iteration and was intentionally omitted to ensure that it was not affected by the much larger errors contributed by the A and X scale factors.

It is interesting to note that during the spin-up calibration, the A and C gyro scale factors were not highly correlated. This was most likely due to the combined effects of lower spin rates and increased spin axis wobble at the lower rates, both of which increase the observability of the individual contributions of these gyros to the propagation errors. These initial values provided an excellent starting point for the subsequent calibrations to be performed, for which the correlation of these scale factors is expected to be much higher because only differential corrections should be required for the remainder of the mission.

The effect of the control axis scale factor calibration is illustrated in Figures 1a, 1b, and 2. Figures 1a and 1b show a histogram of Fine Aspect observation residuals before and after the full calibration for 1,170 stars observations on December 18, 1989, with the temperature effect discussed in Section 3.2 included for both runs. For Figure 1a, the X-axis scale factor was adjusted by hand to minimize the average drift rate, and nominal control axis scale factors were used; the full calibration parameter set was used for Figure 1b. The overall reduction in the residuals is clear, with the RMS reduced from 0.031° to 0.020°. Perhaps more importantly, the full calibration dramatically reduced the number of observations with residuals greater than 0.05° (the Fine Aspect requirement), and the overall distribution is much more Gaussian.

In addition to the Fine Aspect residuals, another sensitive measure of the gyro propagation accuracy is the continuity of the attitude at the boundaries between propagation intervals. Figure 2 shows the discontinuities between attitude intervals before and after the calibration; the average discontinuity was reduced by more than half, from 0.16° to 0.07°.

The independent determination of the spin axis and scale factor is useful in that there is enough variation in the spin rate (from 0.80 to 0.83 RPM) to set a minimum accuracy level for the scale factor itself. This parameter can then be fixed for the remainder of the mission, and any residual spin axis rate errors can be absorbed by the bias term.

Gyro Calibration During Normal Operations

As discussed in the previous section, the requirement for the ground segment gyro calibration activities during the COBE mission phase is twofold: to null the average azimuth drift rate by computing the spin axis bias to high accuracy and to compute differential corrections to the control axis gyros to minimize any pitch rate propagation errors. The spin axis gyro temperature correction is expected to account for most of the drift rate errors observed during the first year of the mission, so the bias corrections are also expected to be small.

As of this writing, the ground segment gyro calibration had not yet been performed for the entire first year of the mission, so only a few test cases have been performed. An illustration of the mission calibration procedure was provided by processing a segment of data from December 1989, a few weeks after the spin-up. The a priori values for this calibration were the final results of the spin-up calibration, and the weights for the solve-for parameters were once again set at unity. The convergence for this calibration was very rapid, using the same convergence criteria as before, so there was no need to adjust the state weights. The results were as follows:

	X Bias (deg/sec)	A Scale Factor	C Scale Factor
Initial	5.2E-4	1.96E-3	-0.46E-3
Final	3.2E-4	1.68E-3	-0.78E-3

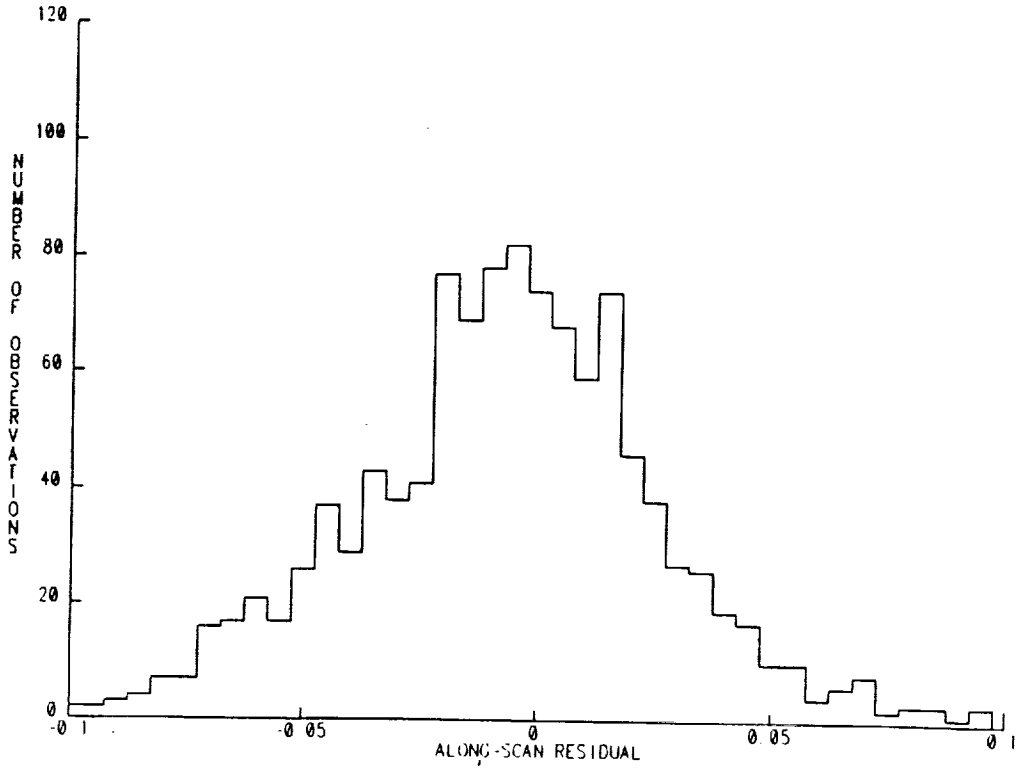

Figure 1a. Fine Aspect Residuals With X-Axis Calibration Only

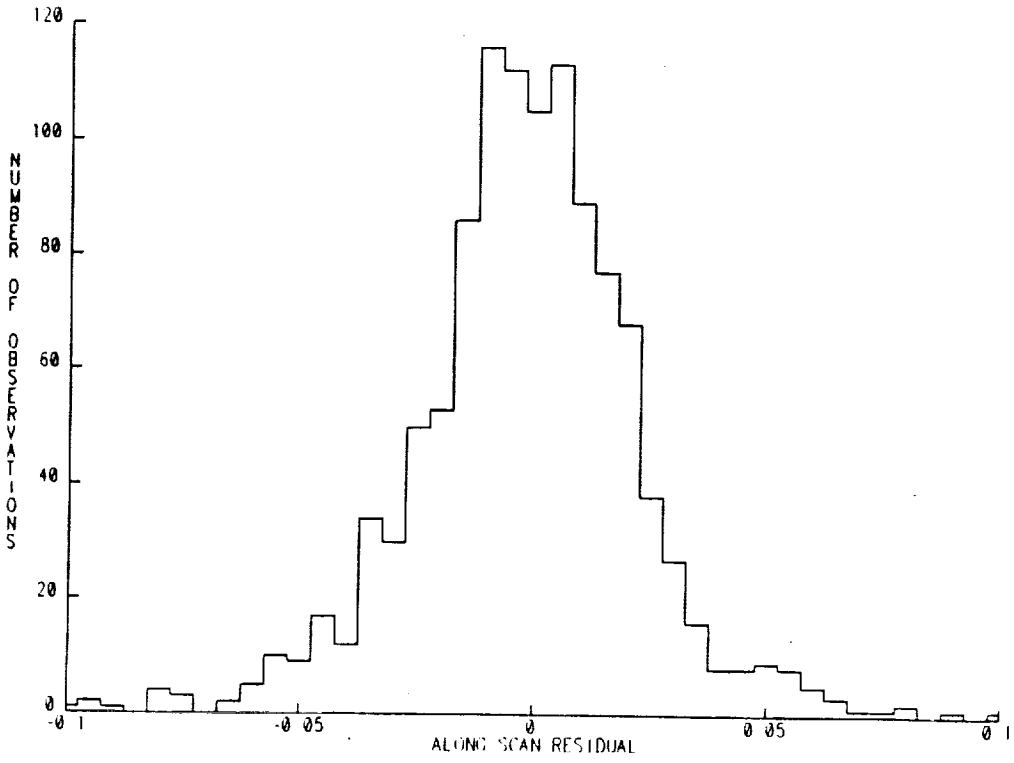

Figure 1b. Fine Aspect Residuals with Full Gyro Calibration

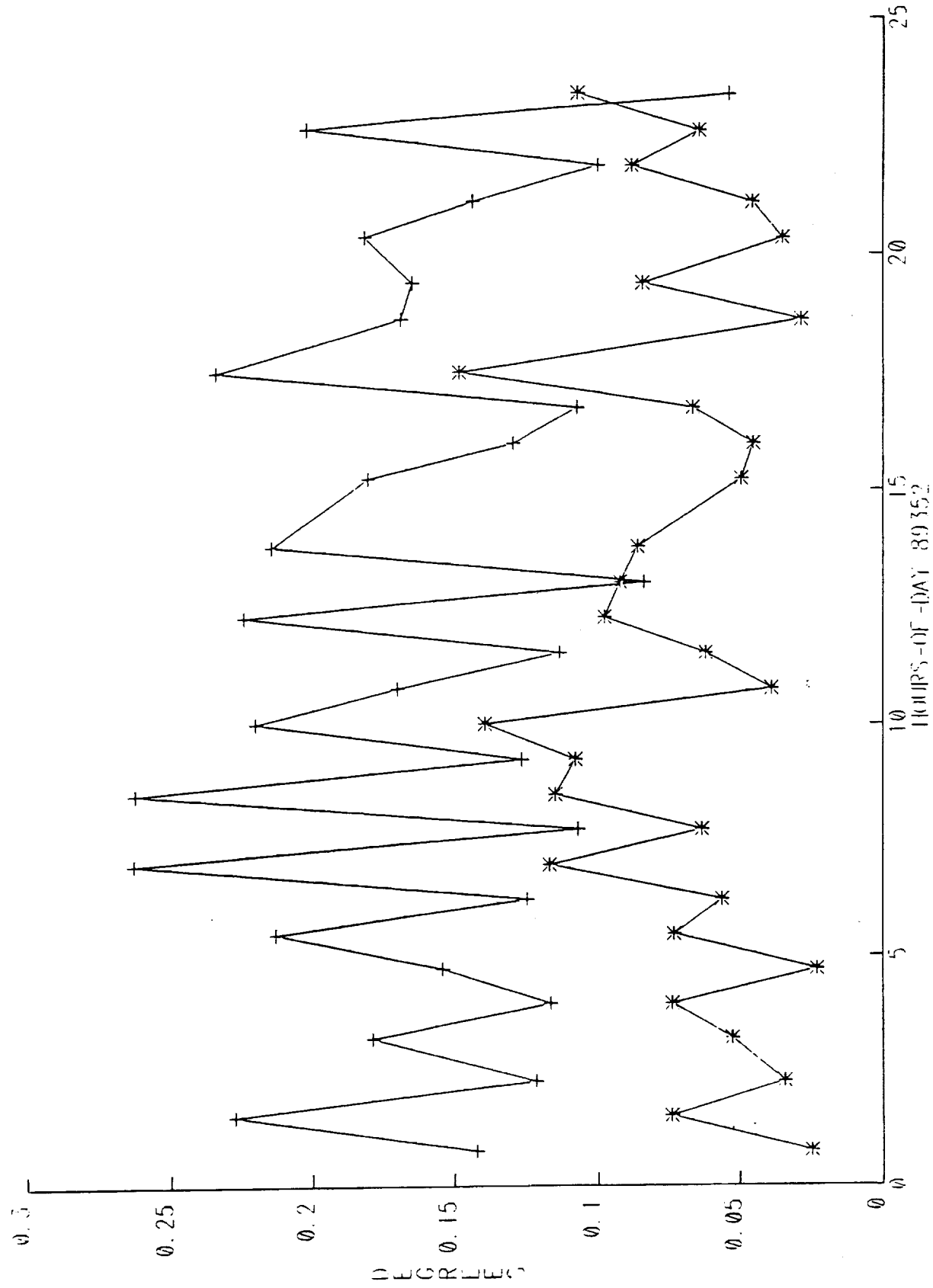

Figure 2. Attitude Discontinuities Before and After Calibration

These results illustrate the correlation of the control gyro scale factors because the corrections to each were nearly the same. Nonetheless, the corrections succeeded in minimizing the pitch component of the propagation errors. The success of this calibration can be judged by the fact that the Fine Aspect solution for this time period produced RMS observation residuals of 1.2 arcminutes, vs. a 3-arcmin accuracy requirement. Thus we conclude that this approach will be very effective for the entire COBE mission, barring any gyro anomalies.

3.2 TEMPERATURE CORRECTION

For most of the first year of the COBE mission, the gyro-propagated attitudes demonstrated cyclic drift rate errors about the spacecraft X axis. The cycle had an orbital and a diurnal component and varied with the spacecraft-commanded roll attitude. The orbital peak-to-peak drift rate errors were typically 1° per hour. This effect could not be attributed to an error in any of the gyro calibration terms and was large enough at times to affect the ability of the DIRBE Fine Aspect system to meet the 3-arcmin requirement.

In addition to this short-term effect, the spin axis drift rates showed considerable variation over the course of the mission. For operational processing these were corrected by manual adjustments of the X-axis gyro scale factor, as discussed in Section 2.1. The scale factor corrections ranged from approximately 0.8E-3 to 1.34E-3, corresponding to variations in drift rate of over 20° per hour.

The effect can be most clearly seen by comparison of the gyro-smoothed coarse attitude with the single-frame coarse attitude. The single-frame attitudes are noisy but reasonably free of long-term systematic errors; the gyro-smoothed attitudes are smooth but show the effects of propagation errors.

To illustrate the various effects of orbital frequency and spacecraft attitude, we have chosen a day that included spacecraft roll slews (December 18, 1989, which included slews from the nominal 4° to 8° and 2° at intervals of a few orbits). The X-axis calibration was chosen to minimize the average drift rate. The gyro-smoothed attitudes were integrated for 45 minutes. Figures 3a through 3c show the azimuth (X-axis), roll, and pitch components of the gyro-smoothed vs. single-frame comparison on this day. The azimuth and roll plots clearly show the variations in the gyro propagation errors over the course of the day.

The cause of this effect was discovered during a test run on the December 18 data. The observed drift variations prompted an investigation of possible external causes for the drift rate variations. A cursory examination of the gyro baseplate temperatures, available from the spacecraft telemetry data base, revealed that they also had an orbital cycle and varied according to the spacecraft roll angle. The effect of the roll slews was to increase the temperature range to about 4°. It was a simple matter to show that the azimuth drift rate errors correlated extremely well with the baseplate temperatures. The temperature variations are shown in Figure 4a, and the correlation of drift rate with temperature on this day is shown in Figure 4b.

After extensive analysis of correlation between the baseplate temperature and the drift rate, the following conclusions were reached: the effect was consistent throughout the mission, it was linear over the observed range of temperatures (15–25 °C), the temperature appeared to affect the gyro scale factor rather than the bias term (at the level of 76 PPM per °C), and there was a time lag of roughly 10 telemetry major frames (320 seconds) between the temperature and drift rate variations.

The CDAC Attitude pipeline software was modified to include a linear temperature correction to the gyro rates, with the linear coefficients and the time delay specified as input parameters. One implementation issue was that the temperature telemetry digitization was fairly coarse (about 0.38 °C); this was resolved by including polynomial smoothing in the correction algorithm. Figure 4a shows both the raw (plotted points) and smoothed (continuous line) temperatures.

This correction, in conjunction with the overall gyro calibration, reduced the typical gyro azimuth propagation error rates to 0.1° per hour. Figures 5a, 5b, and 5c show the single-frame vs. gyro-propagated differences with the temperature correction applied. The correction reduced the typical propagation error to less than the noise in the single-frame solutions in azimuth and roll. The Fine Aspect observation residuals with all corrections applied were

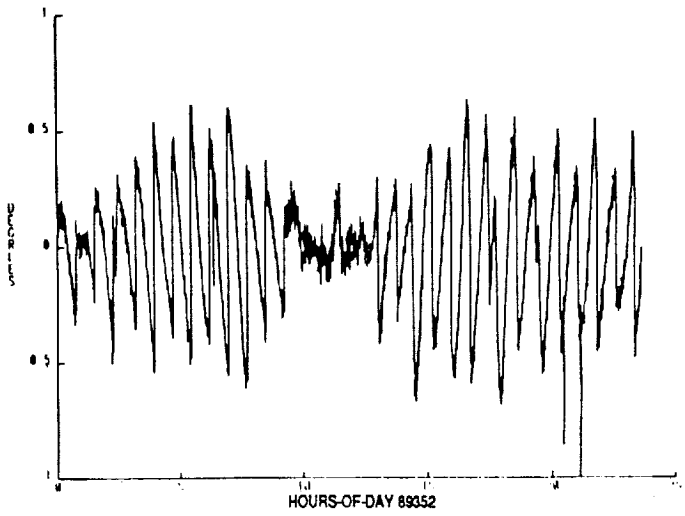

Figure 3a. Gyro Propagation Errors Without Temperature Correction: Azimuth

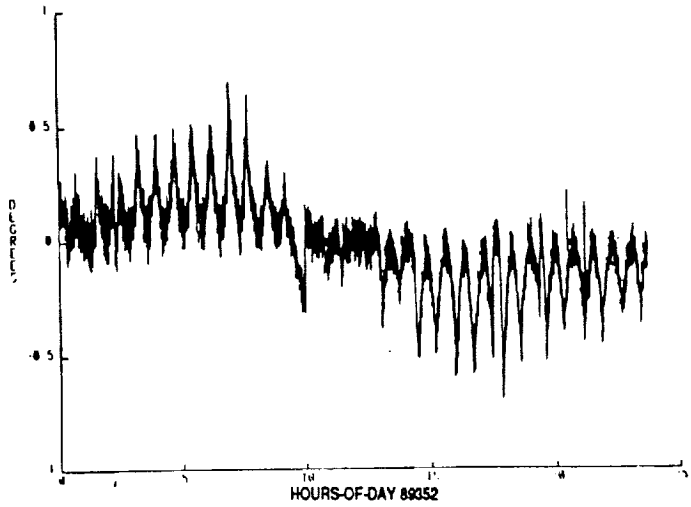

Figure 3b. Gyro Propagation Errors Without Temperature Correction: Roll

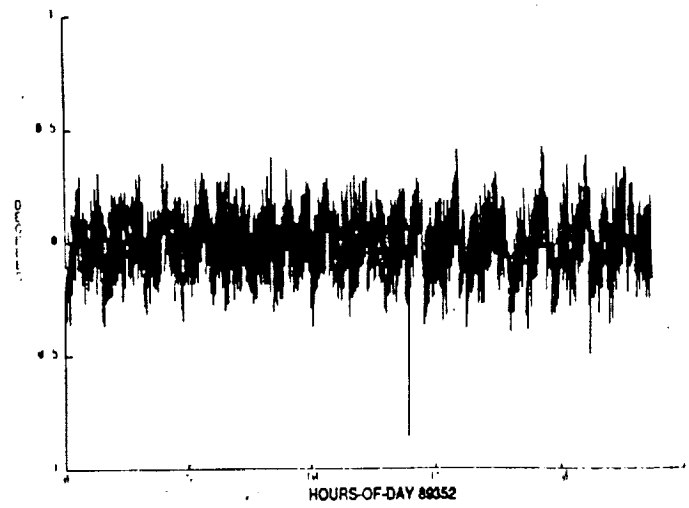

Figure 3c. Gyro Propagation Errors Without Temperature Correction: Pitch

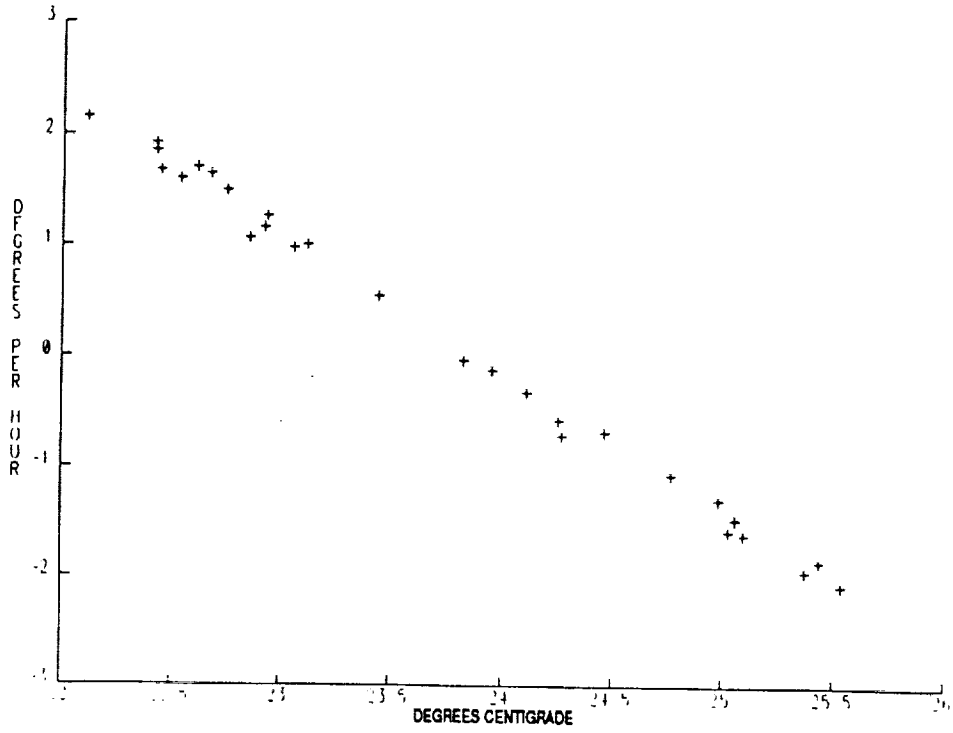

Figure 4a. Azimuth Drift Rate Vs. Gyro Temperature

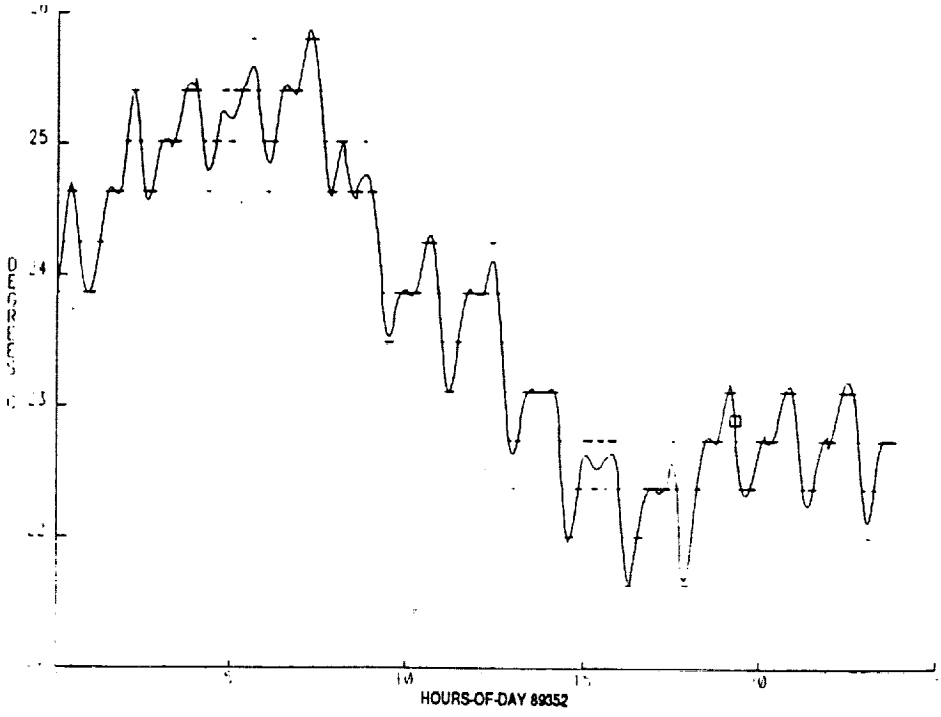

Figure 4b. Raw and Smoothed Gyro Baseplate Temperature

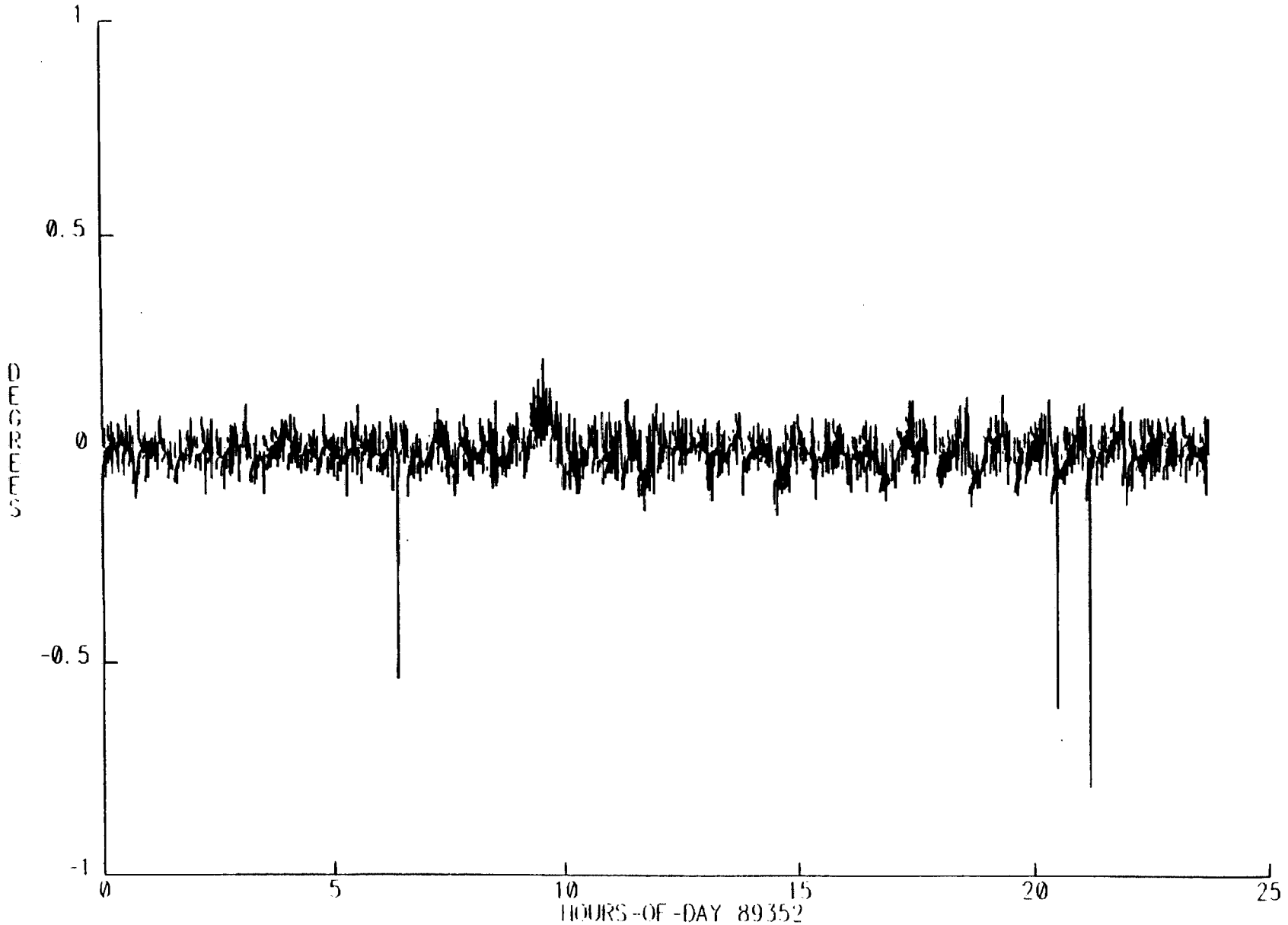

Figure 5a. Gyro Propagation Errors With Temperature Correction: Azimuth

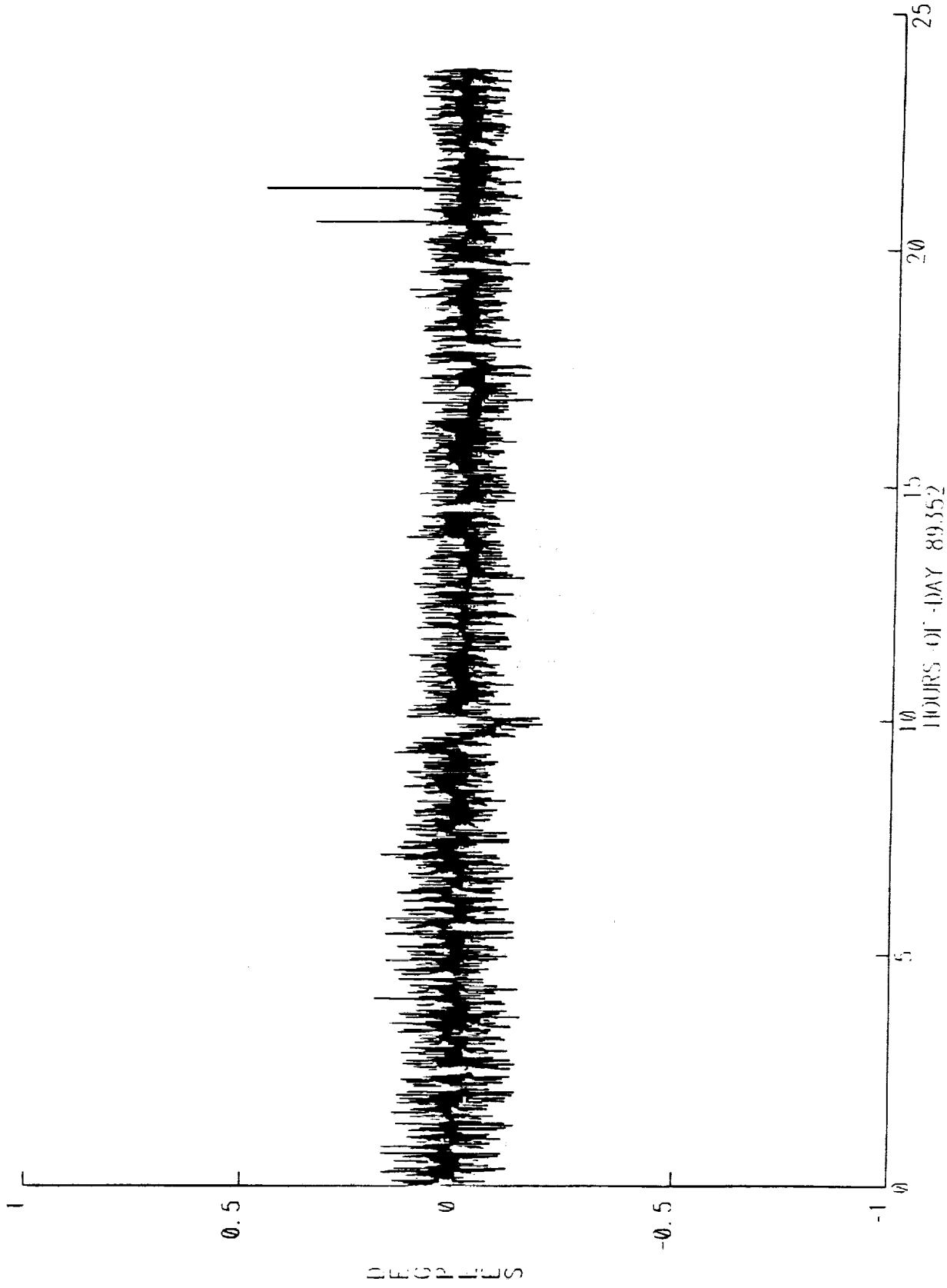

Figure 5b. Gyro Propagation Errors With Temperature Correction: Roll

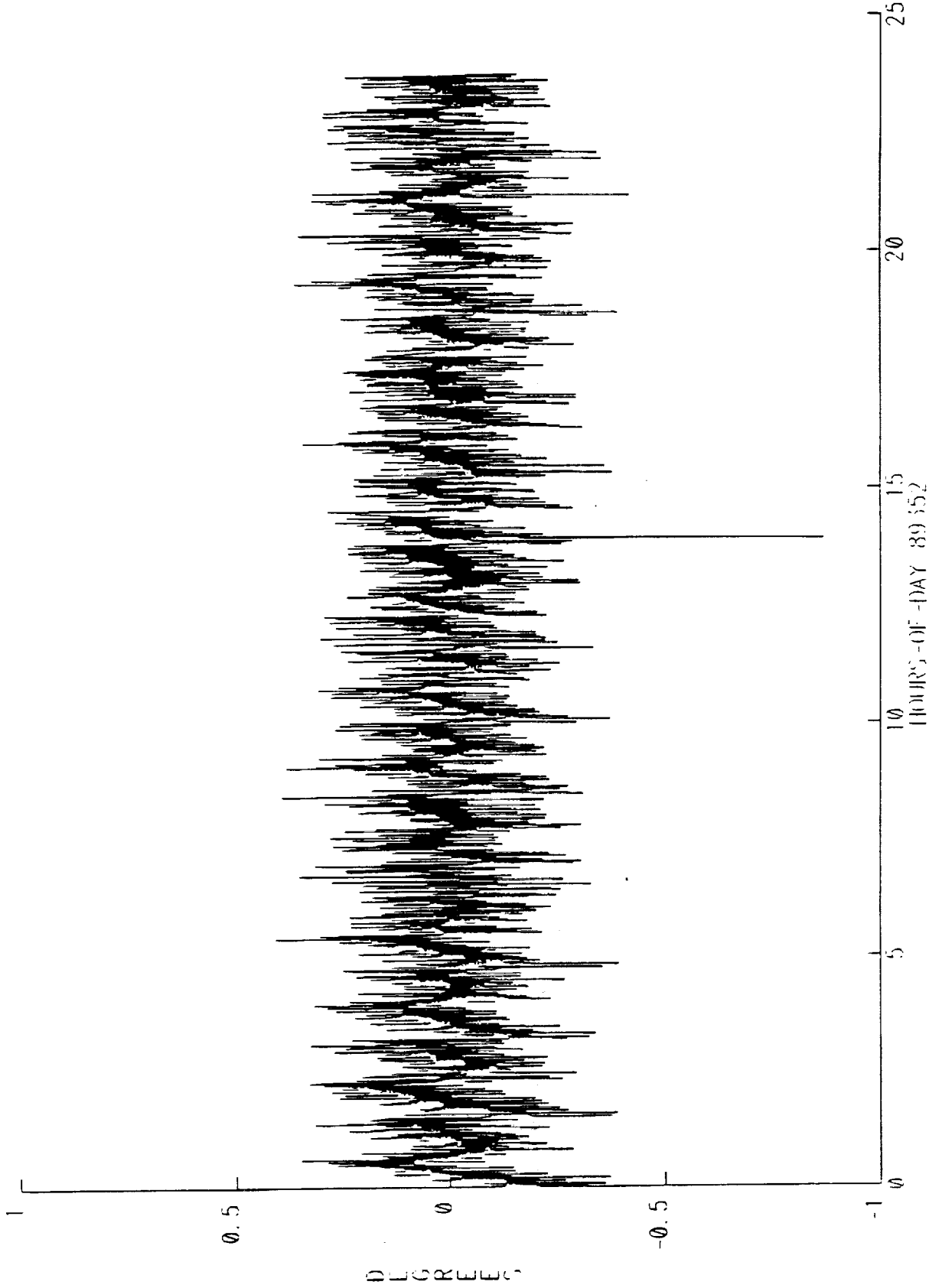

Figure 5c. Gyro Propagation Errors With Temperature Correction: Pitch

reduced from 3 arcminutes RMS using 20-min propagations to less than 1.5 arcminutes using 45-min propagations. After the correction was incorporated into the COBE Science Data Room (CSDR) Attitude operational procedures, the apparent X-axis gyro calibration remained stable for approximately 3 months.

In summary, the characterization of the X-axis gyro temperature effect unlocked the full performance potential of the COBE ground segment gyro calibration and the Fine Aspect system.

4.1 QUALITY ASSURANCE

The operational scenario includes a human intervention step so that the quality of the calibration may be checked before use in the Attitude Pipeline. The quality assurance procedures rely on the plots as shown in the figures to verify the improvement in the aspect solution quality:

- Figure 1 shows the Fine Aspect residual distribution with X-axis calibration only and with full calibration, which includes the control axis gyros.
- Figure 2 shows the attitude discontinuities before and after full calibration.
- Figures 3 and 5 show the single-frame vs. gyro-propagated attitude differences in azimuth, roll, and pitch errors, before and after the temperature correction.

In addition to its support of aspect determination in the production environment, the gyro calibration is an effective diagnostic tool. The best example of this is its recent use to document an instability in the spin-axis gyro for 20 days from Day 16 of 1991. This gyro had been replaced by a backup unit at the time of writing.

4.2 PERFORMANCE RESULTS

Typical results are 120 CPU seconds and 280 I/O operations on a moderately loaded VAX 8800 to process 8 hours of attitude data with 12-min calibration intervals containing attitude samples at 1-sec intervals.

The performance was optimized by storing each full interval of propagated attitude solutions in memory and minimizing the I/O operations.

This implementation is fast enough for closed loop calibration to become possible—the Gyro Calibrator may write a file of partial results per interval that the Pipeline Gyro Propagator may read, especially if a gyro is unstable on the scale of a calibration interval.

SUMMARY AND CONCLUSIONS

This algorithm has been adapted for use on a mission with a unique attitude profile and in an environment where the reference attitudes result from the same system as the propagated attitudes. The gyro calibration results have enabled the overall aspect system to consistently exceed specifications by a comfortable margin, and the implementation has produced an efficient and flexible calibration capability.

ACKNOWLEDGEMENTS

The National Aeronautics and Space Administration/Goddard Space Flight Center (NASA/GSFC) is responsible for the design, development, and operation of the Cosmic Background Explorer (COBE) under the guidance of the COBE Science Working Group. GSFC is also responsible for the development of the analysis software and for the production of the mission data sets.

Special thanks are due to the scientists and engineers who designed and built the DIRBE and to the staff in the attitude control systems branch at GSFC.

REFERENCES

1. Algorithm for In-Flight Gyroscope Calibration," P.B. Davenport and G.L. Welter, NASA Goddard Space Flight Center Flight Mechanics and Estimation Theory Symposium, 1988.

2. "Solar Maximum Mission Attitude System Functional Specifications and Requirements," Computer Sciences Corporation, CSC/SD-68/6082.

3. "COBE Ground Segment Attitude Determination," V.K. Kumar et al., NASA Goddard Space Flight Center Flight Mechanics and Estimation Theory Symposium, 1991.

FLIGHT MECHANICS/ESTIMATION THEORY SYMPOSIUM

MAY 21-23, 1991

SESSION 3